Neutron-proton scattering. II. Spin correlation parameter $A_{yy}(\theta)$ at 50 MeV

D. H. Fitzgerald,* F. P. Brady, R. Garrett,† S. W. Johnsen,‡ J. L. Romero, T. S. Subramanian, J. L. Ullmann, and J. W. Watson§

Crocker Nuclear Laboratory and Department of Physics, University of California, Davis, California 95616

(Received 12 February 1979)

We report on our remeasurement of the n-p scattering observable $A_{yy}(\theta)$, in which 50 MeV (lab) polarized neutrons were scattered from a polarized proton target. Several improvements to the target system have enabled us to greatly reduce the normalization uncertainty in A_{yy}, compared to our earlier measurement. Incorporating these results in a phase shift analysis yields the results $\bar{\delta}(^1P_1) = -6.4° \pm 1.1°$ and $\bar{\epsilon} = 3.6° \pm 1.0°$, where $\bar{\epsilon}_1$ is the $^3S_1$-$^3D_1$ mixing parameter.

[NUCLEAR REACTIONS ^{1}H$(n,p)n$, E_n= 50.0 MeV; measured A_{yy} (θ) from 108° to 174° c.m.]

INTRODUCTION

In recent years, there has been a great deal of interest in the value obtained for the $^3S_1$-$^3D_1$ phase mixing parameter $\bar{\epsilon}_1$ in phase shift analyses[1-4] of n-p scattering data near 50 MeV. The importance of $\bar{\epsilon}_1$ lies in its relation to the n-p tensor force as manifested, for example, in the $^3S_1$-$^3D_1$ admixture in the deuteron and in the deuteron quadrupole moment. It has been shown[2] that the total and differential cross sections and polarization measurements have little direct sensitivity to $\bar{\epsilon}_1$ at 50 MeV. Accordingly, $\bar{\epsilon}_1$ was very poorly determined in early analyses[1,2] of n-p scattering data, which consisted only of these observables. However, the spin-correlation parameter $A_{yy}(\theta)$ was found[2] to be sensitive to $\bar{\epsilon}_1$, and this fact has motivated the measurements of $A_{yy}(\theta)$ to be described here. The parameter $A_{yy}(\theta)$ also shows some sensitivity to the $^1P_1$ phase shift[2]; however, it has been shown[1,3,5] that $\bar{\delta}(^1P_1)$ depends strongly on which differential cross-section data near 50 MeV are included in the phase shift analysis.

We have made two independent sets of measurements of $A_{yy}(\theta)$ at 50.0 MeV, by observing the scattering of polarized neutrons from a polarized proton target. The first measurements,[6] hereafter referred to as $A_{yy}^{(I)}(\theta)$, contained a large normalization uncertainty due to the uncertainty in the proton target polarization. Phase shift analyses[3,4] which included the $A_{yy}^{(I)}(\theta)$ measurements produced fairly well-determined values of $\bar{\epsilon}_1$ at 50.0 MeV. However, these values disagree by one or more standard deviations with those predicted by most models. Further, the experimental and model values for $\bar{\delta}(^1P_1)$ did not agree.

EXPERIMENT

A. Polarized proton target

The polarized proton target consists of a (1% Nd) $La_2Mg_3(NO_3)_{12}24\ H_2O$ hexagonal crystal (commonly called LMN) of 2 mm thickness and 25 mm diameter. Free hydrogen in the waters of hydration is polarized dynamically; this technique is well described in the literature (e.g., see Refs. 7 and 8). A schematic diagram of our system is shown in Fig. 1. The crystal is bathed in supercooled (1.4 °K) ^{4}He and a magnetic field of about 18.8 kG is applied, transverse to the crystal z axis. The polarization at thermal equilibrium (TE), on the basis of Boltzmann statistics, is 0.13%. The polarization is enhanced by applying microwave power (at a frequency near 71 GHz) to

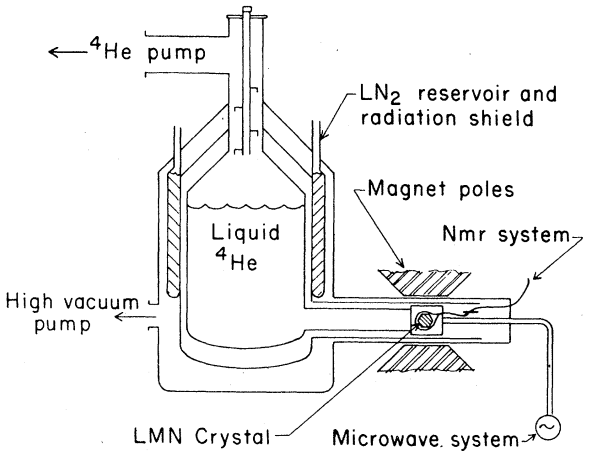

FIG. 1. Schematic diagram of the polarized proton target system.

the crystal and inducing transitions which simultaneously flip the spins of the Nd^{3+} ions and the protons through their dipole-dipole coupling. By a small change in the magnetic field (40 G) the enhanced polarization may be chosen to be parallel or antiparallel to the TE polarization direction. The relative polarization of the crystal is monitored by means of an rf coil wound around the crystal to observe the proton nuclear magnetic resonance (NMR), which occurs at a frequency of about 80 MHz in our case. The absolute polarization then is obtained from the ratio of the TE and enhanced NMR signals. Polarizations in the range between 20 and 50% have been obtained for our system. During the scattering experiment runs, a PDP-11/40 computer and interactive CAMAC system were used to control the operation of the NMR circuit and to collect the NMR data.[9]

For the $A_{yy}^{(I)}$ measurement, the low sensitivity of the NMR circuit and a poor signal-to-noise ratio resulted in an uncertainty of about 25% in the determination of the TE NMR signal size. Subsequently, the rf coil configuration was changed, sources of mechanical vibration and electrical noise were removed, and the NMR circuit was electrically isolated. A dramatic improvement in sensitivity and signal-to-noise ratio resulted from these changes. Accordingly, the average uncertainty in the TE signal size for the present measurement was 2.4%, while that for the enhanced signal was 1.2%. However, the run-to-run dispersion in the enhanced-to-TE-signal ratio was 6.3%, apparently due to long term instability in the NMR circuit. The overall polarization uncertainty was obtained by adding this dispersion in quadrature with (a) a 2.2% uncertainty in the absolute TE polarization, arising from uncertainty in determining the crystal temperature, and (b) a 2.3% uncertainty in determining the correction[10,11] to the enhanced signal magnitude, to account for the dispersion term in the magnetic susceptibility of the LMN crystal. The resulting target polarization uncertainty was 7%, i.e., the proton polarization averaged 0.284 ± 0.020.

B. Polarized neutron beam

As indicated in Fig. 2, a 38.0 MeV deuteron beam, typically at an intensity of 12 μA, is incident on a liquid-nitrogen-cooled cell containing approximately 10^3 Ci of tritium gas at 5.5 atm pressure. Neutrons from the $T(d,\vec{n})\,^4$He reaction, emitted at 29.7° (lab) with an energy of 50.0 MeV (lab) are collimated to form a partially polarized, 24 mm diameter beam with an average intensity of 3×10^4 n/sec in the peak at the polarized proton target.[12] The quantization ($\hat{z}$) axis is taken along

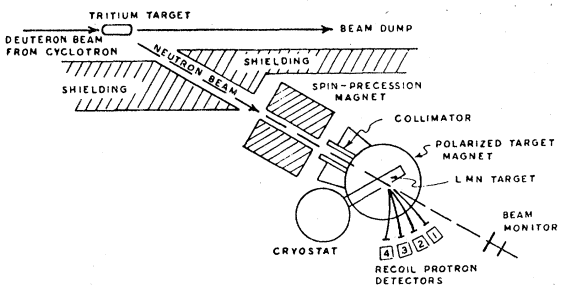

FIG. 2. Schematic diagram of the experimental apparatus, including the polarized neutron production facility, the polarized proton target system, and the detector arrangement.

the neutron beam direction and the $\hat{y}$ axis is taken normal to the scattering plane. The neutron beam polarization has been measured to be 0.476 ± 0.017,[13] using a method proposed by Barschall.[14] The spin-precession magnet shown in Fig. 2 was used during the experiment to reverse the beam polarization. Further details of the neutron beam line are given in Ref. 12.

The neutron beam flux was monitored by placing a thin polyethylene sheet in the beam, downstream from the polarized proton target, and detecting the forward angle recoil protons in a series of three NE 102A plastic scintillators. The neutron beam peak was separated from the low energy tail by time-of-flight (TOF) between a deuteron beam pickoff and the first element of the neutron monitor. The beam peak had a full width at half maximum (FWHM) of 0.6 MeV and a mean energy which has been confirmed to be (50.0 ± 0.1) MeV by a TOF technique. A secondary monitor of the beam flux was provided by deuteron beam current integration.

C. Scattering measurement

Recoil charged particles from reactions in the LMN crystal emerged (at forward angles) through a 0.08 mm thick brass window in the cavity containing the crystal, a 0.008 mm thick aluminum window in the thermal shield which surrounds the ^{4}He cryostat, and a 0.025 mm thick stainless steel window in the cryostat vacuum vessel. As a result, detection of the recoil protons from n-p scattering is limited to forward angles (backward neutron scattering angles) where the protons have sufficient energy to be detected. The energy spread of the recoil protons and their orbits in the polarizing magnetic field, for a given initial recoil angle, were calculated using a computer code[15] which integrated the proton initial position over the volume of the crystal and took account of the proton energy loss in materials in the

flight path. For protons recoiling to the right of 0° (toward the detectors in Fig. 2) the energy spread for a given initial angle varied from 4.4 to 6.8 MeV for the lab recoil angles in this experiment (0°–37°). Protons recoiling to the left of 0° had considerably greater energy losses in the LMN crystal and various windows. The correspondingly large energy spread which was observed in a trial run during the experiment precluded left-right asymmetry measurements.

Four ΔE-E telescopes were used to detect charged particles, as shown in Fig. 2. Each of the two forward angle telescopes consisted of 4.6 cm wide by 10.2 cm high plastic scintillator (NE 102A) elements of thickness 0.15 cm for ΔE and 2.5 cm for E. The corresponding dimensions for the backward angle telescopes were 5.1 cm (width) by 10.2 cm (height) by 0.10 cm thick (ΔE) and 1.3 cm thick (E). Including the effect of the crystal diameter, each telescope subtended a polar lab angle of approximately 6°. Recoil protons from n-p scattering were detected at angles corresponding to average c.m. neutron scattering angles of 108°, 130°, 156°, and 174°.

Fast timing signals, measured relative to the deuteron beam pickoff, were derived from each E detector photomultiplier anode. The overall resolution of the system varied from 5.4 MeV, at 0° recoil angle, to 8.5 MeV, at 37° recoil angle, due mainly to the proton energy spread at the detectors. The analog and timing signals were processed electronically and transferred, using a CAMAC interface, to an on-line PDP 15/40 computer. All data were recorded, event-by-event, on magnetic tape for later off-line analysis.

Data were taken for all four possible combinations of neutron and proton spins, parallel to the $\hat{y}$ axis. The pulse-height distribution of the nontarget background for each detector was determined from earlier runs[15] with the LMN crystal removed. No convenient method could be found to determine the nonhydrogen background contribution from the LMN crystal. However, as shall be seen, uncertainties in determining the background have a small effect on the uncertainty in $A_{yy}(\theta)$.

DATA ANALYSIS AND RESULTS

In an off-line analysis, the data were played back from magnetic tape and, for each detector, displayed in a ΔE vs E spectrum. Soft-ware restrictions were used to separate protons from other types of charged particles. For proton events, further restrictions on a TOF (relative to the beam pickoff) vs E spectrum were used to remove events due to neutrons in the low energy beam tail. Figure 3 shows an example, for θ_n (c.m.) = 156°,

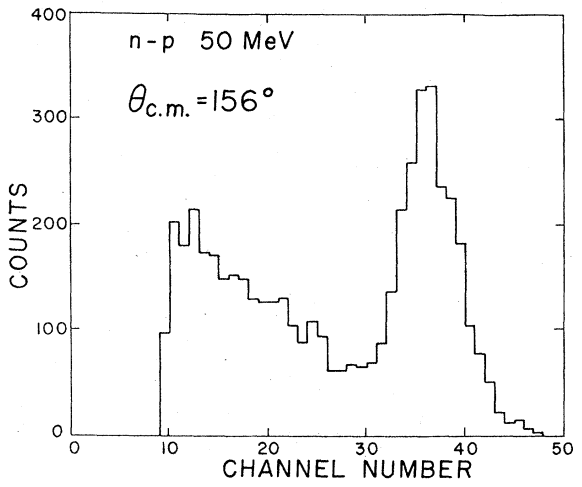

FIG. 3. Pulse height spectrum for recoil protons detected at an angle corresponding to a neutron c.m. scattering angle of 156°, and subject to particle identification and TOF restrictions, as explained in the text.

of the proton spectra which were obtained as a function of pulse height, subject to these restrictions.

Detector gain shifts during the experiment were negligible. Therefore, for a given detector, the two-parameter software cuts were identical for all runs for all four target and beam spin orientations. Likewise, no evidence was seen for dependence of the background spectra on target or beam spin orientation, and so the assumed background under the elastic scattering peak was identical for all runs for a given detector.

The background spectrum for a given detector was estimated in the following fashion. The earlier target-out measurement showed the nontarget background to be featureless. Its magnitude accounted for 60–90% of the yield in target-in spectra except, of course, in the region of the elastic scattering peak. Accordingly, the background contribution due to (n,p) reactions on the nonhydrogen components of the LMN crystal was assumed to be small and the total background spectrum under the elastic peak was assumed to be smooth. The magnitude of the background under the peak was estimated by a fit to the observed background on either side of the peak, assuming first a linear shape and later a parabolic shape, in separate analyses of all the data. For the former analysis, the peak yield was determined from counts above background, and for the latter, both counts above background and a Gaussian fit to the peak were used. From a comparison of the yields obtained by these methods, the worst case uncertainty in determining the background for a single run was estimated to range from 1% of the

yield at θ_n(c.m.) = 174° to 5% at θ_n(c.m.) = 180°. This uncertainty was included with the statistical uncertainty for the peak yield, which was taken to be that determined from counts above a linear background.

For the case of beam and target polarized along the y axis and the final spin states not observed, the scattering angular distribution is given by[16]

$$I(\theta, P_b, P_t) = I_0(\theta)[1 + (P_b + P_t)A_y(\theta) + P_b P_t A_{yy}(\theta)]. \quad (1)$$

$I_0(\theta)$ is the (unpolarized) n-p differential cross section, $A_y(\theta)$ is the analyzing power, and P_b and P_t are the beam and target polarizations, respectively. The measured values of $I(\theta, P_b, P_t)$ for the four different spin orientations may be combined, using Eq. (1), to yield

$$A_{yy} = (|P_b||P_t|)^{-1} \frac{(\uparrow\uparrow) - (\uparrow\downarrow) + (\downarrow\downarrow) - (\downarrow\uparrow)}{(\uparrow\uparrow) + (\uparrow\downarrow) + (\downarrow\downarrow) + (\downarrow\uparrow)}. \quad (2)$$

Note that this combination not only eliminates the need for knowing $I_0(\theta)$ and $A_y(\theta)$, but also substantially reduces the contribution of systematic uncertainties. For example, the uncertainty in background subtraction is eliminated in the numerator, at least to first order.

Approximately 25 hours of useful data were obtained at four angles for each spin combination. The dispersion in the run-to-run yields agreed very well with that expected on the basis of Poisson statistics. Therefore, the uncertainty in the total yields was calculated from counting statistics and background subtraction uncertainty. This overall statistical uncertainty in $I(\theta)$ ranged from 1.3% at θ_n(c.m.) = 174° to 2.0% at θ_n(c.m.) = 108°.

$A_{yy}(\theta)$ was calculated at each angle using Eq. (2); the results appear in Table I. The uncertainties shown in the table do not include the overall normalization uncertainty, which is 7.8%, arising from uncertainties in the beam (3.6%) and target (7%) polarizations. The present results are also compared with the $A_{yy}^{(I)}(\theta)$ values in Fig. 4. In this figure, the experimental values of $A_{yy}^{(I)}(\theta)$ and $A_{yy}^{(II)}(\theta)$ have been multiplied by normalization factors of 1.23 and 1.07, respectively, obtained in a phase shift analysis.[3] As can be seen, the agreement between the $A_{yy}^{(I)}(\theta)$ values and the present results is quite good; on the average, the statistical uncertainties for the present results are 70% of those for $A_{yy}^{(I)}(\theta)$. The significant improvement in the present results, compared to $A_{yy}^{(I)}(\theta)$, however, is not shown in the figure. That is, the 26% normalization uncertainty for the $A_{yy}^{(I)}(\theta)$ data has been reduced to 7.8% for the present results, as a result of an improved measurement of the target polarization. The absolute target and beam polarization determine the slope of $A_{yy}(\theta)$ data at backward angles; i.e., an increase in P_t or P_b makes the slope of $A_{yy}(\theta)$ less negative for $100° \leq \theta_n$(c.m.) $\leq 180°$.

TABLE I. $A_{yy}(II)$.

$\theta_{c.m.}$	$A_{yy}(\theta_{c.m.})$
108°	+0.241 ± 0.071
130°	+0.189 ± 0.072
156°	−0.037 ± 0.051
174°	−0.194 ± 0.054

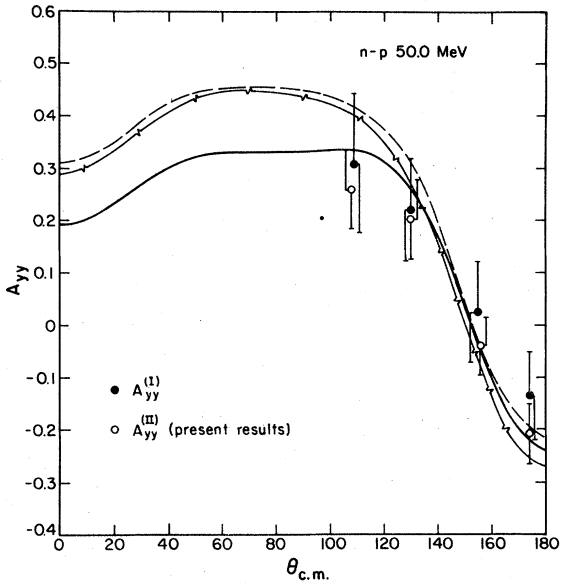

FIG. 4. Angular distributions for the $A_{yy}^{(I)}(\theta)$ measurements (solid dots) and the present $[A_{yy}^{(I)}(\theta)]$ measurements (open circles). The curves are present phase shift analysis (solid curve), and OBEP model predictions, as described in the text: Ref. 23 (dashed curve) and Ref. 24 (broken curve).

As a check on the values used for P_b and P_t, the analyzing power, $A_y(\theta)$, was calculated from the measured yields for the four spin orientations, using Eq. (1) to obtain two expressions for $A_y(\theta)$, in terms of the yields and either P_t or P_b. That is, at each θ, two values for $A_y(\theta)$ were obtained by averaging over either the beam or target polarization. The values obtained are shown in Table II. As can be seen, the two values are in good agreement at each angle, and no systematic difference between the values is apparent. These $A_y(\theta)$ data also agree, well within statistics, with phase shift results[3] and with earlier data from Harwell[17] and Davis,[18] also shown in Table II.

DISCUSSION

In a 1974 paper,[2] Binstock and Bryan discussed the sensitivity of various n-p scattering ob-

TABLE II. Comparison of $A_y(\theta_{c.m.})$.

	Present results				
$\theta_{c.m.}$	$A_y(\theta_{c.m.})$ [a]	$A_y(\theta_{c.m.})$ [b]	$A_y(\theta_{c.m.})$ [c]	$A_y(\theta_{c.m.})$, $\theta_{c.m.}$ [d]	$A_y(\theta_{c.m.})$, $\theta_{c.m.}$ [e]
108°	0.063 ± 0.071	0.084 ± 0.071	0.113	0.095 ± 0.011, 109.3°	0.105 ± 0.012, 109°
130°	0.026 ± 0.072	0.048 ± 0.072	0.059	0.058 ± 0.008, 129.4°	0.062 ± 0.010, 129°
156°	0.024 ± 0.051	0.007 ± 0.051	0.018	0.014 ± 0.013, 149.6°	0.007 ± 0.014, 158.5°
174°	0.001 ± 0.054	0.009 ± 0.054	0.003		

[a] Averaged over incident neutron spin.
[b] Averaged over target proton spin.
[c] Reference 3 phase shift results.
[d] Reference 18.
[e] Reference 17.

servables at 50 MeV to a change in one of seven phase parameters. In particular, they found that $A_{yy}(\theta)$ was sensitive to $\bar{\delta}(^1P_1)$ and especially to $\bar{\epsilon}_1$. Although other observables, such as A_{zz} and C_{pp}, are somewhat more sensitive to $\bar{\epsilon}_1$ than is A_{yy}, these measurements entail considerably greater experimental difficulty than does A_{yy}.

The inclusion of the $A_{yy}^{(I)}$ data in phase shift analyses of n-p and p-p scattering data substantially reduced the uncertainty in $\bar{\epsilon}_1$. However, in two separate analyses, the values obtained at 50 MeV, $\bar{\epsilon}_1 = 0.2° \pm 1.7°$ (Refs. 3 and 6) and $\bar{\epsilon}_1 = -0.92° \pm 2.19°$ (Ref. 4), respectively, were lower than the (positive) 2–3° resulting from most calculations based on models of the two-nucleon interaction. Even for the analysis of Ref. 6, negative values of $\bar{\epsilon}_1$ could not be ruled out at 50 MeV. Further, the value obtained for $\bar{\epsilon}_1$ was found[3] to depend strongly on the differential cross-section data used in the analysis, apparently in conflict with the result of Binstock and Bryan,[2] who found little change in $\sigma(\theta)$ for a 3° change in $\bar{\epsilon}_1$. This effect, as well as the dependence of $\bar{\delta}(^1P_1)$ near 50 MeV on various cross-section data sets, will be discussed in a later paper.[19]

These results strongly suggested that the determination of $\bar{\epsilon}_1$ and $\bar{\delta}(^1P_1)$ could be improved by (a) an independent measurement of $\sigma(\theta)$ near 60 MeV, and (b) additional measurements of $A_{yy}(\theta)$ at 50 MeV with reduced uncertainties. The former measurement has been carried out recently and is reported in the preceding paper.[20] The latter measurement, reported here, represents a reduction of statistical uncertainties by 30%, on the average, and a reduction of the normalization uncertainty by a factor of 3.3, compared to the $A_{yy}^{(I)}(\theta)$ data. These new data, together with new Davis $A_y(\theta)$ data[18] at 50 MeV, total cross sections[21] at 49.1, 54.4, and 59.4 MeV, differential cross sections[22] at 50 MeV, $A_y(\theta)$ data[17] at 50 and 60 MeV and the $A_{yy}^{(I)}(\theta)$ data,[6] formed the n-p data base for a phase shift analysis, which yields, at $E_n = 50$ MeV, the values $\bar{\epsilon}_1 = 3.6° \pm 1.0°$ and $\bar{\delta}(^1P_1) = -6.4° \pm 1.1°$. The resulting prediction for $A_{yy}(\theta)$ is shown as the solid curve in Fig. 4.

Compared to the results of earlier analyses, these values are in much better agreement with values obtained in model-dependent analyses. The $A_{yy}(\theta)$ distributions for two model-dependent calculations are also shown in Fig. 4. These are (a) a one-boson-exchange-potential (OBEP) model of Bryan and Gersten[23] ("model C": $\bar{\epsilon}_1 = 2.78°$, $\bar{\delta}(^1P_1) = -8.76°$), shown as a dashed curve, and (b) an OBEP model, with asymptotic power law energy dependence, of Ueda and Green[24] ("model IV", $\bar{\epsilon}_1 = 2.40°$, $\bar{\delta}(^1P_1) = -10.24°$), shown as a broken curve.

As part of a general investigation[19] of phase shift parameters near 50 MeV, the dependence of $\bar{\epsilon}_1$ and $\bar{\delta}(^1P_1)$ on the n-p data base has been studied extensively. For the data set indicated above, which includes the present $A_{yy}(\theta)$ and 63.1 MeV differential cross section[20] measurements, the addition of other differential cross-section data[25] now causes $\bar{\epsilon}_1$ and $\bar{\delta}(^1P_1)$, respectively, to vary by less than a standard deviation. Details of this study will be forthcoming. General conclusions which can currently be drawn are that as a result of the new measurements of $A_{yy}(\theta)$ and $\sigma(\theta)$[20] negative values of $\bar{\epsilon}_1$ near 50 MeV are ruled out, the values obtained for $\bar{\epsilon}_1$ and $\bar{\delta}(^1P_1)$ show markedly better stability than formerly, and the agreement of these phase parameters with model values has improved.

ACKNOWLEDGMENTS

The authors are indebted to Professor P. Signell for extensive discussions of the phase shift analysis results and for a critical reading of the manuscript. This work was supported by Grant No. PHY77-05301 of the National Science Foundation.

*Present address: LAMPF Visitors Center MS 831, Los Alamos Scientific Laboratory, Los Alamos, N. M. 87545.
†Permanent address: University of Auckland, Auckland, New Zealand.
‡Present address: Varian Corporation, Palo Alto, Calif.
§Present address: Kent State University, Physics Department, Kent, Ohio 44242.

[1]R. A. Arndt, J. Binstock, and R. Bryan, Phys. Rev. D 8, 1397 (1973).
[2]J. Binstock and R. Bryan, Phys. Rev. D 9, 2528 (1974).
[3]Peter Signell (private communication).
[4]R. A. Arndt, R. H. Hackman, and L. D. Roper, Phys. Rev. C 15, 1021 (1977).
[5]Ronald Bryan and Judith Binstock, Phys. Rev. D 10, 72 (1974).
[6]S. W. Johnsen, F. P. Brady, N. S. P. King, M. W. McNaughton, and Peter Signell, Phys. Rev. Lett. 38, 1123 (1977).
[7]C. D. Jeffries, *Dynamic Nuclear Orientation* (Interscience, New York, 1963).
[8]T. J. Schmugge and C. D. Jeffries, Phys. Rev. 138, A1785 (1965).
[9]S. W. Johnsen, Nucl. Instrum. Methods 116, 269 (1974).
[10]John J. Hill and Daniel A. Hill, Nucl. Instrum. Methods 116, 269 (1974).
[11]V. Petricek, Nucl. Instrum. Methods 58, 111 (1968).
[12]A. L. Sagle, M. W. McNaughton, N. S. P. King, F. P. Brady, and B. E. Bonner, Nucl. Instrum. Methods 129, 345 (1974).
[13]A. L. Sagle, M. W. McNaughton, N. S. P. King, B. E. Bonner, and F. P. Brady, in *Few Body Problems in Nuclear and Particle Physics, Quebec, 1974,* edited by R. J. Slobodrian, B. Cujec, and K. Ramavataram, (Les Presses de l'Université Laval, Quebec, 1975); A. L. Sagle *et al.* (unpublished); and Report No. UCD-CNL 190.
[14]H. H. Barschall, Helv. Phys. Acta 29, 149 (1956).
[15]S. W. Johnsen, Ph.D. thesis, U. C. Davis (1975).
[16]J. Raynal, Nucl. Phys. 28, 220 (1961); N. Hoshizaki, Prog. Theo. Phys. Suppl. 42, 107 (1968).
[17]A. Langsford, P. H. Bowen, G. C. Cox, G. B. Huxtable, and R. J. Riddle, Nucl. Phys. 74, 241 (1965).
[18]J. L. Romero, M. W. McNaughton, F. P. Brady, N. S. P. King, T. S. Subramanian, and J. L. Ullmann, Phys. Rev. C 17, 468 (1978).
[19]D. H. Fitzgerald, N. S. P. King, F. P. Brady, and P. Signell (unpublished).
[20]N. S. P. King, J. D. Reber, J. L. Romero, D. H. Fitzgerald, J. L. Ullmann, T. S. Subramanian, and P. F. Brady, preceding paper, Phys. Rev. C 21, 1185 (1980).
[21]F. P. Brady, W. J. Knox, J. A. Jungerman, M. R. McGie, and R. L. Walraven, Phys. Rev. Lett. 25, 1628 (1970).
[22]T. C. Montgomery, F. P. Brady, B. E. Bonner, W. B. Broste, and M. W. McNaughton, Phys. Rev. C 16, 499 (1977).
[23]R. A. Bryan and A. Gersten, Phys. Rev. D 6, 341 (1974).
[24]T. Ueda and A. E. S. Green, Phys. Rev. C 18, 337.
[25]M. J. Saltmarsh, C. R. Bingham, M. L. Holbert, C. A. Lindeman, and A. van der Woude, Oak Ridge National Laboratory (unpublished). A table of the data is given in Ref. 1.